

Defect of the Five-Thirds Law Using the Wiener–Hermite Expansion

Tung-chen Chung^{1,2} and William C. Meecham¹

Received July 6, 1988; revision received January 17, 1989

Application of the refined Wiener–Hermite expansion with moderate to high Reynolds numbers Re to homogeneous, isotropic turbulence is presented. The results show a defect to Kolmogorov’s “five-thirds law,” increase in the absolute value of the exponent comparable with many theoretical predictions. Midrange spectra up to fluctuation Reynolds numbers of 10^8 show little, if any, dependence of the defect on Re , as long as the initial spectra do not deviate too far from their equilibrium states. The renormalization scheme has also been proven to have no effect on the final shape of the spectrum.

KEY WORDS: Wiener–Hermite expansion; Kolmogorov’s five-thirds law; energy spectrum; energy dissipation fluctuation; defect.

1. INTRODUCTION

The influence of the intermittency of the kinetic energy dissipation (see ref. 1) on Kolmogorov’s “five-thirds law” for the velocity spectrum $E(k)$ in the inertial subrange, $1/L \ll K \ll 1/\eta$, L the outer scale and η the dissipation length was first noted in ref. 2 some time after the formulation of Kolmogorov’s theory.⁽³⁾ Many authors have worked on this question since then.^(4–7)

The quantity

$$\varepsilon = 0.5\nu(\partial u_i/\partial x_j + \partial u_j/\partial x_i) \quad (1)$$

is a random variable undergoing considerable fluctuation in space and time, where ν is the kinematic viscosity and u_i, u_j are the components of the velocity field $\mathbf{u}(\mathbf{x}, t)$. For this reason (as has been shown in the

¹ Mechanical, Aerospace and Nuclear Engineering Department, University of California, Los Angeles, California 90024.

² Smith, Fause & Associates, Culver City, California 90230.

above references), the Kolmogorov five-thirds law deduced using simple dimensional analysis cannot be exact. Deviation from the five-thirds law originating from the intermittence of the energy dissipation is slight and is difficult to determine experimentally. However, it should be possible to calculate it analytically with a proper theory.

2. REVIEW OF WIENER-HERMITE EXPANSION

We use the Wiener-Hermite (WH) expansion, which has been used successfully to treat decaying, homogeneous and isotropic turbulence.⁽⁸⁾

The central idea of the WH theory is to expand the turbulent velocity field (or any random quantity) with respect to a complete set of stochastic functionals such that the first term in the expansion has Gaussian statistics and higher order terms represent deviations from Gaussianity. The expansion is in essence one about Gaussianity designed to take advantage of the nearly Gaussian (in many ways) nature of turbulence.⁽⁹⁾ Two basic advantages of the WH expansion should be emphasized: the results are necessarily realizable (all energy spectra are positive) and the theory is deductive, using no adjustable or quasiempirical parameters or functions.

The basic element of the Wiener-Hermite expansion is the white noise process. Consider a scalar function $H^{(1)}(x)$ of a scalar variable defined as follows. Divide the x axis into cells of width Δ . The value of $H^{(1)}$ in each cell is selected independently from a Gaussian distribution with a variance Δ^{-1} . As we let $\Delta \rightarrow 0$, $H_{\Delta}^{(1)}(x)$ approaches $H^{(1)}(x)$, the idealized, one-dimensional, white noise process.

This can be easily extended to the three-dimensional vector case by replacing the cells of width Δ by cells of volume Δ^3 , the variance Δ^{-1} by Δ^{-3} , and the process $H^{(1)}(x)$ by the vector $H_i^{(1)}(\mathbf{x})$. This vector has the following properties:

$$\begin{aligned} \langle H_i^{(1)}(\mathbf{x}) \rangle &= 0 \\ \langle H_i^{(1)}(\mathbf{x}) H_j^{(1)}(\mathbf{x}') \rangle &= \delta_{ij} \delta(\mathbf{x} - \mathbf{x}') \\ &\vdots \end{aligned} \tag{2}$$

with δ_{ij} the Kronecker delta and $\delta(\mathbf{x})$ the Dirac delta function.

A physical random process $u_i(\mathbf{x})$ which has a Gaussian distribution can be written as

$$u_i(\mathbf{x}) = \int K_{i\alpha}^{(1)}(\mathbf{x}, \mathbf{x}') H_{\alpha}^{(1)}(\mathbf{x}') d\mathbf{x}' \tag{3}$$

where $K_{ix}^{(1)}(\mathbf{x}, \mathbf{x}')$ is a “nonrandom” function, and summation on repeated indices is implied. The correlation tensor of u_i is

$$\langle u_i(\mathbf{x}) u_j(\mathbf{x}') \rangle = \int K_{ix}^{(1)}(\mathbf{x}, \mathbf{x}'') K_{jx}^{(1)}(\mathbf{x}', \mathbf{x}''') d\mathbf{x}'' d\mathbf{x}''' \tag{4}$$

When the process is statistically homogeneous, $K_{ix}^{(1)}(\mathbf{x}, \mathbf{x}')$ can be written as $K_{ix}^{(1)}(\mathbf{x} - \mathbf{x}')$.

For a non-Gaussian process we define polynomial combinations of the white noise process in such a way that they are mutually, statistically orthogonal. The first few are

$$\begin{aligned} H_x^{(0)}(\mathbf{x}) &= 1 \\ H_{\alpha\beta}^{(2)}(\mathbf{x}_1, \mathbf{x}_2) &= H_x^{(1)}(\mathbf{x}_1) H_\beta^{(1)}(\mathbf{x}_2) - \delta_{\alpha\beta} \delta(\mathbf{x}_1 - \mathbf{x}_2) \\ H_{\alpha\beta\gamma}^{(3)}(\mathbf{x}_1, \mathbf{x}_2, \mathbf{x}_3) &= H_x^{(1)}(\mathbf{x}_1) H_\beta^{(1)}(\mathbf{x}_2) H_\gamma^{(1)}(\mathbf{x}_3) \\ &\quad - H_x^{(1)}(\mathbf{x}_2) \delta_{\beta\gamma} \delta(\mathbf{x}_2 - \mathbf{x}_3) \\ &\quad - H_\beta^{(1)}(\mathbf{x}_2) \delta_{\gamma\alpha} \delta(\mathbf{x}_3 - \mathbf{x}_1) - H_\gamma^{(1)}(\mathbf{x}_3) \delta_{\alpha\beta} \delta(\mathbf{x}_1 - \mathbf{x}_2) \\ &\quad \vdots \end{aligned} \tag{5}$$

Statistical orthogonality means that

$$\langle H^{(m)} H^{(n)} \rangle = 0 \quad \text{for } m \neq n \tag{6}$$

Each functional also has zero statistical mean:

$$\langle H^{(m)} \rangle = 0 \tag{7}$$

A statistically homogeneous random process which has zero mean and is not Gaussian can be written in terms of Wiener–Hermite functionals as follows:

$$\begin{aligned} u_i(\mathbf{x}) &= \int K_{ij}^{(1)}(\mathbf{x} - \mathbf{x}') H_j^{(1)}(\mathbf{x}') d\mathbf{x}' \\ &\quad + \iint K_{ijl}^{(2)}(\mathbf{x} - \mathbf{x}', \mathbf{x} - \mathbf{x}'') H_j^{(2)}(\mathbf{x}', \mathbf{x}'') d\mathbf{x}' d\mathbf{x}'' + \dots \end{aligned} \tag{8}$$

If the process does not deviate greatly from Gaussian form, there exists an expansion which converges quickly. The velocity field of a turbulent fluid is generally of this kind. But, for rigid convergence, it is necessary to alter the choice of the white noise process at later times.

For homogeneous turbulence it is convenient to work in wavenumber space. We define the Fourier transform of a velocity field $u_i(\mathbf{x})$ as

$$u_i(\mathbf{k}) = \int d\mathbf{x} u_i(\mathbf{x}) \exp(i\mathbf{k} \cdot \mathbf{x}) \tag{9}$$

In this representation $\mathbf{u}(\mathbf{k})$ becomes

$$u_i(\mathbf{k}) = K_{ij}^{(1)}(\mathbf{k}) H_j^{(1)}(\mathbf{k}) + (2\pi)^{-3} \int K_{ijl}^{(2)}(\mathbf{k} - \mathbf{k}', \mathbf{k}') H_{jl}^{(2)}(\mathbf{k} - \mathbf{k}', \mathbf{k}') d\mathbf{k}' + \dots \tag{10}$$

For more details see ref. 8.

If we take the Fourier transform of the Navier–Stokes equation, we get

$$(\partial/\partial t + \nu k^2) u_i(\mathbf{k}, t) = (2\pi)^{-3} iP_{ij}(\mathbf{k}) k_l \int u_j(\mathbf{k} - \mathbf{q}, t) u_l(\mathbf{q}, t) d\mathbf{q} \tag{11}$$

where

$$P_{ij}(\mathbf{k}) = \delta_{ij} - k_i k_j / k^2 \tag{12}$$

Perform the following steps: (a) substitute the equation for $\mathbf{u}(\mathbf{k})$, Eq. (10), into the Navier–Stokes equation in wavenumber space, keeping only the first two terms of order $(K^{(2)})$, assuming that the turbulence is, in a sense, nearly Gaussian; through (b) multiply the resulting equation by $H^{(1)}$ and take the ensemble average; (c) multiply the equation from part (a) by $H^{(2)}$ and take the ensemble average. From (b) and (c) we have coupled differential equations for $K^{(1)}$ and $K^{(2)}$, respectively. In these two equations there are terms containing $\dot{H}^{(1)}$ and $\dot{H}^{(2)}$, which will be specified later.

For incompressible, homogeneous, isotropic turbulence, the first kernel $K_{ij}^{(1)}(\mathbf{k})$ can be written in terms of a scalar generator $U(k)$:

$$K_{ij}^{(1)}(\mathbf{k}) = U(k) P_{ij}(\mathbf{k}) \tag{13}$$

If we further assume that the turbulence is exactly Gaussian at time $t = 0$, the second kernel can at all later times be written in terms of a single scalar function $F(\mathbf{k}_1, \mathbf{k}_2)$:

$$K_{ijl}^{(2)}(\mathbf{k}_1, \mathbf{k}_2) = i(\mathbf{k}_1 + \mathbf{k}_2)_m P_{im}(\mathbf{k}_1 + \mathbf{k}_2) \{ P_{jm}(\mathbf{k}_1) P_{ln}(\mathbf{k}_2) F(\mathbf{k}_1, \mathbf{k}_2) + P_{jm}(\mathbf{k}_1) P_{ln}(\mathbf{k}_2) F(\mathbf{k}_2, \mathbf{k}_1) \} \tag{14}$$

Consider $\dot{H}^{(1)}$ and $\dot{H}^{(2)}$. The second can be determined once the first is defined. The quantity $\dot{H}^{(1)}$ is just a random process. It can be argued⁽¹⁰⁾ that $\dot{H}^{(1)}$ can be written as

$$\dot{H}_i^{(1)}(\mathbf{k}) = \int L_{ijl}^{(2)}(\mathbf{k} - \mathbf{k}', \mathbf{k}') H_{jl}^{(2)}(\mathbf{k} - \mathbf{k}', \mathbf{k}') d\mathbf{k}' \quad (15)$$

where $L_{ijl}^{(2)}$ has to satisfy a measure-preserving condition. The final form of $L_{ijl}^{(2)}$ is obtained independently in refs. 10 and 11 as

$$L_{ijl}^{(2)}(\mathbf{k}_1, \mathbf{k}_2) = \frac{1}{2}i(2\pi)^{-3} (\mathbf{k}_1 + \mathbf{k}_2)_\alpha P_{i\beta}(\mathbf{k}_1 + \mathbf{k}_2) P_{\beta l}(\mathbf{k}_2) P_{\alpha j}(\mathbf{k}_1) V(k_1) \quad (16)$$

The function $V(k)$ is defined here as $U(k)$, but could more generally be arbitrary. We choose U in order to produce the Gaussian equipartition solution of the inviscid equation, $\nu = 0$. Other choices must be judged by the rapidity of convergence of the representation in particular applications.

The final forms of the equations for the two kernels $K^{(1)}$ and $K^{(2)}$ in terms of the scalar functions U and F are ($y = \cos \theta$, θ the angle between \mathbf{k} and \mathbf{q})

$$\begin{aligned} &(\partial/\partial t + \nu k^2) U(k) \\ &= -(2\pi)^{-2} \int_0^\infty \int_{-1}^1 \{P_4 F(\mathbf{k}, \mathbf{q}) + (P_2 + P_3) F(\mathbf{q}, \mathbf{k})\} dy U(q) q^2 dq \\ &+ (2\pi)^{-2} \int_0^\infty \int_{-1}^1 \{P_2 F(\mathbf{k} + \mathbf{q}, -\mathbf{q}) \\ &+ P_3 F(-\mathbf{q}, \mathbf{k} + \mathbf{q})\} dy \nu(q) q^2 dq \end{aligned} \quad (17)$$

and

$$(\partial/\partial t + |\mathbf{k}_1 + \mathbf{k}_2|^2 \nu) F(\mathbf{k}_1, \mathbf{k}_2) = \frac{1}{2}U(k_1) U(k_2) - \frac{1}{2}U(k_1) U(|\mathbf{k}_1 + \mathbf{k}_2|) \quad (18)$$

where

$$\begin{aligned} P_2 &= k_\alpha k_\beta P_{\gamma\delta}(\mathbf{k}) P_{\gamma\beta}(\mathbf{q}) P_{\alpha\delta}(\mathbf{k} + \mathbf{q}) \\ P_3 &= k_\alpha k_\beta P_{\gamma\delta}(\mathbf{k}) P_{\alpha\beta}(\mathbf{q}) P_{\gamma\delta}(\mathbf{k} + \mathbf{q}) \\ P_4 &= k_\alpha q_\beta P_{\gamma\beta}(\mathbf{k}) \{P_{\alpha\delta}(\mathbf{q}) P_{\gamma\delta}(\mathbf{k} + \mathbf{q}) + P_{\gamma\delta}(\mathbf{q}) P_{\alpha\delta}(\mathbf{k} + \mathbf{q})\} \end{aligned} \quad (19)$$

We can now write out the energy spectrum in terms of $K^{(1)}$ and $K^{(2)}$. The transfer can be shown to be conservative. We let portions of the energy E_1 and E_2 correspond to contributions from $K^{(1)}$ and $K^{(2)}$. They are, loosely speaking, the Gaussian and non-Gaussian parts of the energy.

The moving base $L^{(2)}$ described above gives solutions for short times and moderate Reynolds number only. When t increases, E_2 grows from zero and eventually becomes bigger than E_1 , which violates our Gaussian

approximation. In other words, the expansion is then poorly convergent. Larger Re worsens the situation.

To remedy this, Hogge and Meecham⁽⁸⁾ devised the renormalization procedure. The idea is to use a measure-preserving transformation so that, simultaneously; (1) the energy spectrum is preserved and (2) the size of E_2 and the error in the transfer are minimized. The procedure is as follows: (a) when E_2 becomes too large, the integration is stopped; (b) U is calculated as if all the energy is in E_1 , call it U' ; (c) a form of F is assumed, called F' , with parameters to be determined; (d) E_2 is expressed in terms of F' ; (e) the transfer function $T(k)$ is expressed in terms of U' and F' , called $T'(k)$; (f) the quantity $\Delta^2 = \int \{T(k) - T'(k)\}^2 dk$ is calculated in terms of the parameters for F' ; (g) E_2 and Δ^2 are minimized simultaneously with respect to these parameters, which are evaluated; (h) the F thus found is used to correct U using $E = E_1 + E_2$. The result of these steps is a new set of $\{U, F\}$ defining a measure-preserving transformation which gives smaller E_2 so as to improve the two-term truncation of the WH expansion and preserve the transfer function and the total energy E . Note that we renormalize at fixed times. After the new U and F are obtained, the integration is resumed until E_2 increases again, at which time the renormalization procedure is repeated.

In this work we use a WH expansion with a time-dependent base and with the renormalization scheme to calculate the evolution of the turbulence measured and simulated by the numerical experiment.

3. RESULTS ON THE DEFECT OF THE FIVE-THIRDS LAW USING THE WIENER-HERMITE EXPANSION AND CALCULATIONS

Preliminary results of Chung and Meecham⁽¹²⁾ suggested that for a fluctuation Reynolds number of 1000, all of the initial spectra k^{-1} , $k^{-7/5}$, $k^{-5/3}$, k^{-2} transform to slopes near $-5/3$ (-1.667), but decreased by $+0.12$, approximately. However, there were various indications in this early work that a larger Reynolds number was needed to reach the usual defect.

The Reynolds number was accordingly raised to 10,000, with different initial spectra and renormalized at every second time step. For initial spectra that do not deviate too much from the five-thirds law (between -1.342 and -2.138 in the exponent, see Table I), the resulting slopes were determined by applying linear regression to the fairly straight portion of the energy spectrum in inertial subrange, between wavenumbers 2.000 and 11.314. After a dimensionless time of two (outer scaling of time, $k_0 u_0 t$, throughout), the slopes all fall within a range between -1.691 and -1.728 .

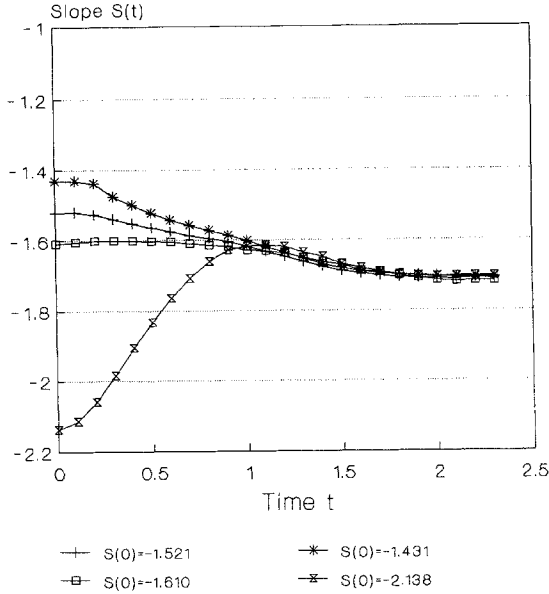


Fig. 1. Slope transition from $t=0.0$ to $t=2.3$. The slope for each initial spectrum $S(0)$ is generated by the generalized Kolmogorov spectrum formula⁽¹⁶⁾ and is taken from the inertial subrange and calculated by least-square fit from $k=2.000$ to $k=11.314$. Reynolds number $Re = 10,000$. (+) $S(0) = -1.521$, (*) $S(0) = -1.431$, (□) $S(0) = -1.610$, (X) $S(0) = -2.138$.

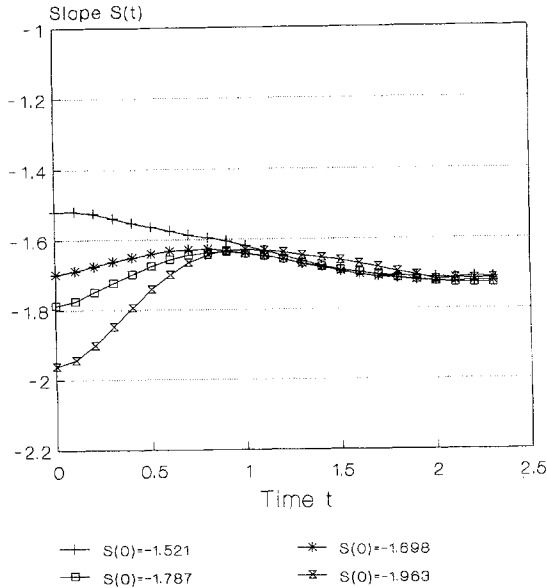


Fig. 2. Slope transition from $t=0.0$ to $t=2.3$. The slope for each initial spectrum is generated by the generalized Kolmogorov spectrum formula⁽¹⁶⁾ and is taken from the inertial subrange and calculated by least-square fit from $k=2.000$ to $k=11.314$. Reynolds number $Re = 10,000$. (+) $S(0) = -1.521$, (*) $S(0) = -1.698$, (□) $S(0) = -1.787$, (X) $S(0) = -1.963$.

That is, there is a decrease of about 0.024 to 0.061 in the exponent of the five-thirds law. For dimensionless time exceeding 1.8, in most cases the slope reaches its (just given) asymptotic value and stays there with but small fluctuation (as the Reynolds number drops at later time).

Various different Reynolds numbers were run with the same initial spectra (and different initial spectra). From a series of results we find that using an equilibrium initial spectrum in the generalized Kolmogorov spectrum formula (actual slope calculated from linear regression in the inertial subrange stated above for this initial spectrum turned out to be -1.521 ; see Table I), between fluctuation Reynolds number 2000 and 10^8 , most of the resulting slopes, after $t = 2$, fall within -1.702 and -1.717 . As a matter of fact, over a wide range of Reynolds numbers, from 2500 to 3000 and from 10,000 to 20,000, the slopes resulting from a $-5/3$ initial spectrum all approach a value of -1.712 , which is about the value of $-5/3 - \mu/9$, a frequently predicted value, as noted above.⁽⁴⁻⁶⁾

For all the spectra in this work, large wavenumbers near the dissipation range, i.e., near k_v are not resolved. The dimensionless wavenumber goes up to about 181, a designated cutoff wavenumber in this calculation. However, it is also shown in the Appendix that this (the cutoff) does not seriously affect the midrange spectral results.

Figures 1-5 show that the slopes of the energy spectra for various runs

Table I. Slopes for Various Reynolds Numbers and Initial Spectra at $t = 2.3$

Re	Slope for given initial spectrum $S(0)$									
	-1.252	-1.342	-1.431	-1.521	-1.609	-1.698	-1.787	-1.963	-2.138	-2.485
1,663				-1.698		-1.623				
2,000				-1.702						
2,500				-1.711						
3,000				-1.713						
5,000				-1.717				-1.727		
10,000	-1.683	-1.696	-1.707	-1.714	-1.721	-1.726	-1.728	-1.726	-1.703	-1.697
12,500				-1.712						
15,000		-1.691		-1.712						
16,600				-1.712		-1.725				
16,630				-1.712						
20,000				-1.711						
100,000				-1.708						-1.615
200,000				-1.708						
500,000		-1.695		-1.707				-1.717		
1,000,000				-1.707						
1.0e + 08				-1.707						

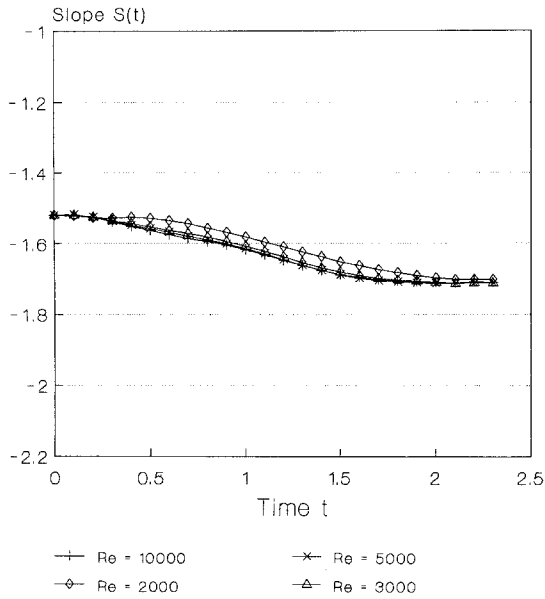


Fig. 3. Slope transition from $t=0.0$ to $t=2.3$. The slope for the initial spectrum is generated by the generalized Kolmogorov spectrum formula⁽¹⁶⁾ $S(0) = -1.521$ and is taken from the inertial subrange and calculated by least-square fit from $k=2.000$ to $k=11.314$. Reynolds number Re is: (+) 10,000, (*) 5000, (Δ) 3000, (\diamond) 2000.

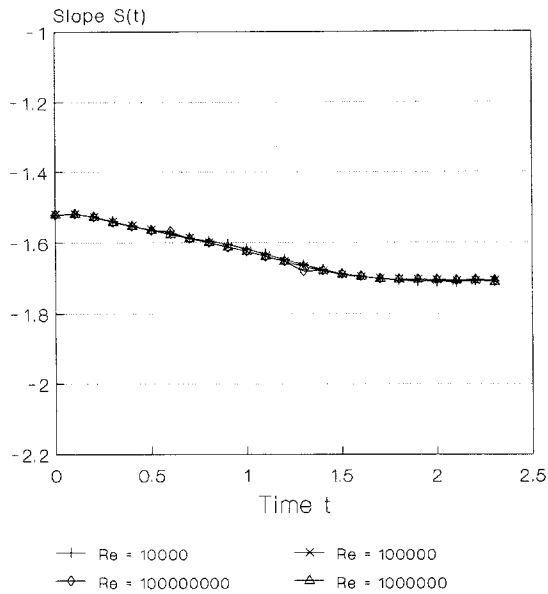


Fig. 4. Slope transition from $t=0.0$ to $t=2.3$. The slope for the initial spectrum is generated by the generalized Kolmogorov spectrum formula⁽¹⁶⁾ $S(0) = -1.521$ and is taken from the inertial subrange and calculated by least-square fit from $k=2.000$ to $k=11.314$. Reynolds number Re is: (+) 10^4 , (*) 10^5 , (Δ) 10^6 , (\diamond) 10^8 .

with different Reynolds numbers and/or different initial spectra approach the value of -1.712 after a dimensionless time of two. Figures 6–10 are energy spectra for various combinations of Reynolds numbers and initial spectra. Figures 1 and 2 show runs with Reynolds number 10^4 but with different initial spectra. Figures 3 and 4 show runs with the same initial spectrum (-1.521 as shown, but entered with $-5/3$ in the Kolmogorov generalized spectrum) and different Reynolds numbers. Note that over a wide range of Reynolds numbers, from about 3000 to 10^8 , the transition of the slope of the energy spectrum does not vary much from run to run. Figures 6 and 7 are energy spectra of runs with the same Reynolds number, 10^4 , but with different initial spectra. Figures 8 and 9 are spectra of runs with the same initial spectrum and different Reynolds numbers. Note that these energy spectra collapse on each other over a large portion of the spectrum curve except at the largest wavenumbers, which proves that the influence of the Reynolds number on the initial subrange is small. Table I lists the slopes after a dimensionless time of two for various runs with different Reynolds numbers and initial spectra.

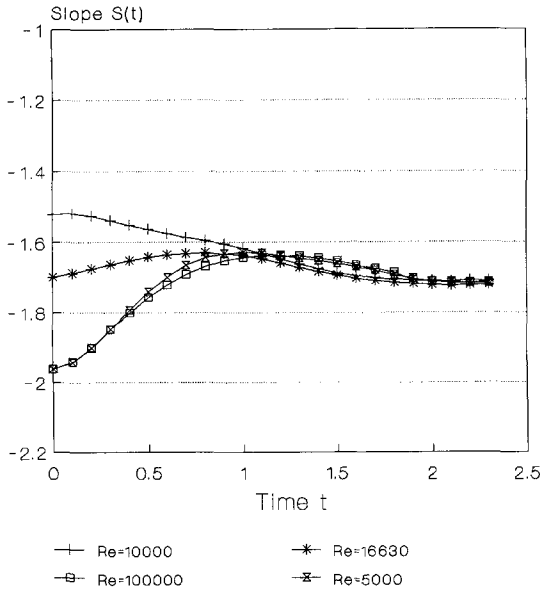


Fig. 5. Slope transition from $t=0.0$ to $t=2.3$. The slope for each initial spectrum is generated by the generalized Kolmogorov spectrum formula⁽¹⁶⁾ and is taken from the inertial subrange and calculated by least-square fit from $k=2.000$ to $k=11.314$. (+) Reynolds number $Re=10,000$, $S(0)=-1.521$; (*) Reynolds number $Re=16,630$, $S(0)=-1.698$; (□) Reynolds number $Re=100,000$, $S(0)=-1.963$; (Σ) Reynolds number $Re=5,000$, $S(0)=-1.963$.

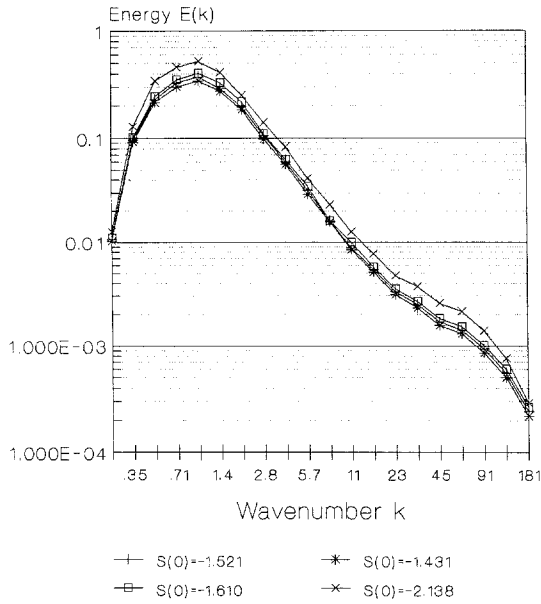


Fig. 6. Energy spectrum at $t=2.3$. The slope for each initial spectrum is generated by the generalized Kolmogorov spectrum formula⁽¹⁶⁾ and is taken from the inertial subrange and calculated by least-square fit from $k=2.000$ to $k=11.314$. Reynolds number $Re=10,000$. (+) $S(0)=-1.521$, (*) $S(0)=-1.431$, (□) $S(0)=-1.610$, (×) $S(0)=-2.138$.

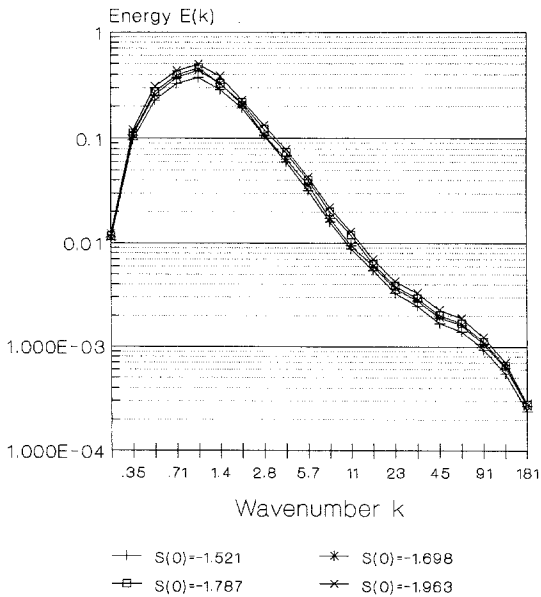


Fig. 7. Energy spectrum at $t=2.3$. The slope for each initial spectrum is generated by the generalized Kolmogorov spectrum formula⁽¹⁶⁾ and is taken from the inertial subrange and calculated by least-square fit from $k=2.000$ to $k=11.314$. Reynolds number $Re=10,000$. (+) $S(0)=-1.521$, (*) $S(0)=-1.698$, (□) $S(0)=-1.787$, (×) $S(0)=-1.963$.

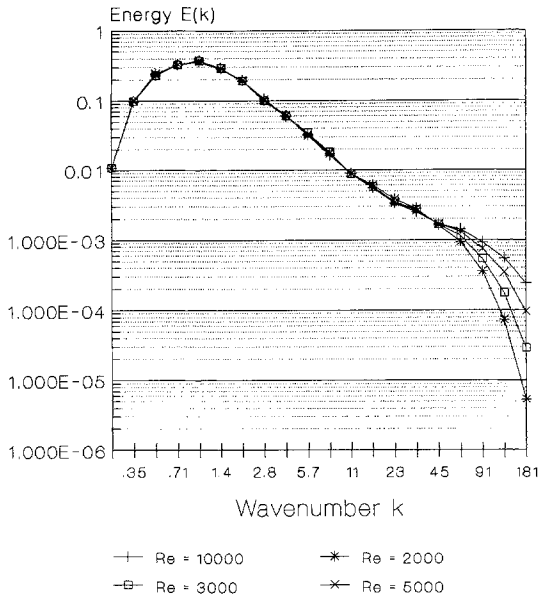


Fig. 8. Energy spectrum at $t = 2.3$. The slope for the initial spectrum is generated by the generalized Kolmogorov spectrum formula⁽¹⁶⁾ $S(0) = -1.521$ and is taken from the inertial subrange and calculated by least-square fit from $k = 2.000$ to $k = 11.314$. Reynolds number Re is: ($+$) $10,000$, ($*$) 2000 , (\square) 3000 , (\times) 5000 .

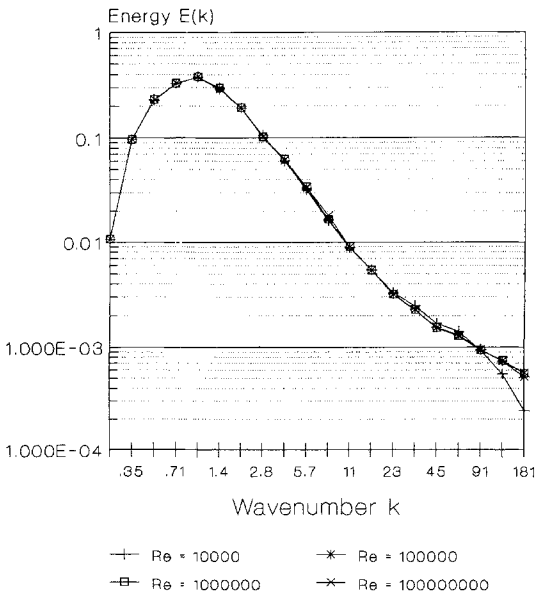


Fig. 9. Energy spectrum at $t = 2.3$. The slope for the initial spectrum is generated by the generalized Kolmogorov spectrum formula⁽¹⁶⁾ $S(0) = -1.521$ and is taken from the inertial subrange and calculated by least-square fit from $k = 2.000$ to $k = 11.314$. Reynolds number Re is: ($+$) 10^4 , ($*$) 10^5 , (\square) 10^6 , (\times) 10^8 .

The above results show a defect in Kolmogorov's five-thirds law very close to what others have predicted,⁽⁴⁻⁷⁾ that is, a decrease of 0.045 in the exponent (an increase in absolute value) from the original five-thirds law. It should be emphasized that the Wiener-Hermite expansion is being severely pushed at a fluctuation Reynolds number of 10^8 (large wavenumbers near the dissipation range were not resolved, as mentioned above), an extremely large value not obtainable using other methods. Nevertheless, we feel that these results are reliable.^(8,9) There is a suggestion that the defect may slightly reduce as decay time increases (fluctuation Reynolds number decreases). From the computed results we also find that the dependence on the initial spectrum is small, although its effect is greater than that of the Reynolds number. In fact, with the same initial spectra, the longer time spectra resulting from different Reynolds numbers coincide with each other over a large spectral region except at the largest wavenumbers. There we may have (WH expansion) truncation error due to higher-order non-Gaussian contributions. Furthermore, and more importantly, for the highest Reynolds numbers, the wavenumber range at and near the dissipation wavenumber is not resolved. This, it is seen, does not

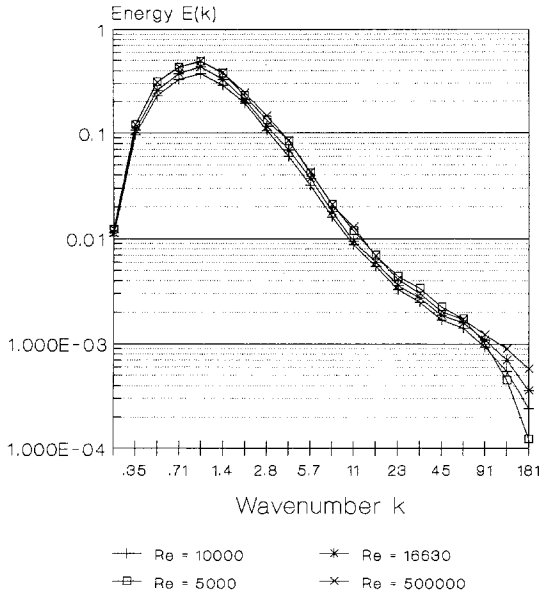


Fig. 10. Energy spectrum at $t = 2.3$. The slope for each initial spectrum is generated by the generalized Kolmogorov spectrum formula⁽¹⁶⁾ and is taken from the inertial subrange and calculated by least-square fit from $k = 2.000$ to $k = 11.314$. (+) Reynolds number $Re = 10,000$, $S(0) = -1.521$; (*) Reynolds number $Re = 16,630$, $S(0) = -1.698$; (□) Reynolds number $Re = 5000$, $S(0) = -1.963$; (×) Reynolds number $Re = 500,000$, $S(0) = -1.963$.

affect midrange spectral values, however. Other cases with different combinations of initial spectra and Reynolds numbers, within the ranges mentioned above also give consistent resulting slopes.

Although we were not able to get comparable results outside the initial spectral values and Reynolds numbers mentioned above (i.e., initial spectra smaller than -1.342 or larger than -2.138 and Reynolds numbers smaller than 1663), we noted that for equilibrium initial spectrum, the Reynolds number can be pushed to as high as 10^8 and the resulting slope only differs slightly from that of the Reynolds number 10^5 . To our knowledge this is the first deductive theory to calculate midrange spectra to such Reynolds numbers.

From a dimensional argument, in order to get a defect from the five-thirds law, we must introduce a parameter other than ε . The only parameters available are those from the energy range, either U (or L) or the viscosity ν . If the latter, the defect would be Reynolds number dependent, but our calculations seem not to support such a dependence: the defect for the most part appears to be independent of Reynolds number. Then, dimensionally we are forced to the conclusion that the

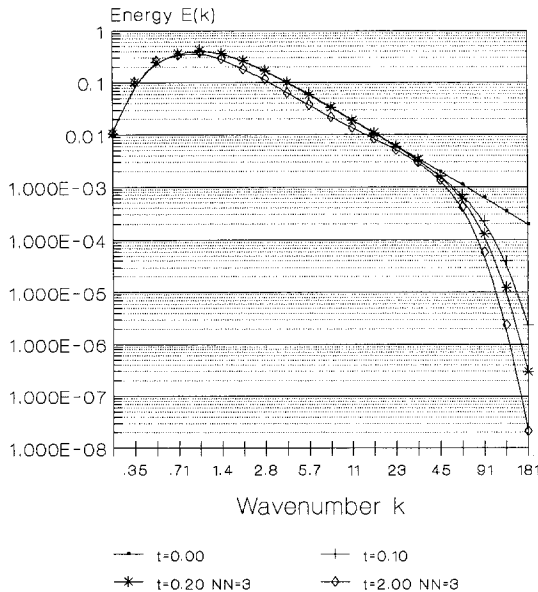


Fig. 11. Energy spectrum at (■) $t = 0.00$, (+) $t = 0.10$, (*) $t = 0.20$, (◇) $t = 2.00$. The slope for the initial spectrum is generated by the generalized Kolmogorov spectrum formula⁽¹⁶⁾ $S(0) = -1.521$ and is taken from the inertial subrange and calculated by least-square fit from $k = 2.000$ to $k = 11.314$. Reynolds number $Re = 1000$. For $t = 0.20$ and $t = 2.00$, NN (the renormalization rate plus 1) is equal to 3, i.e., renormalization occurs at every other time step.

defect, if present, must be due to energy range dependence, presumably a “leapfrogging” of (a small amount of) energy from the energy range into the high-wavenumber range.

One way to actually calculate the leapfrog transfer would be to calculate the function $T(k, k')$ in the asymptotic range for $k \sim k'$, the energy range wave number, and $k' \gg k$; there should be a very small but finite transfer. Since the function of T is itself very small, it would be very difficult to make a reliable calculation of this asymptotic behavior.

The preliminary results of our previous work showed that the deviation in the five-thirds law of the energy spectrum due to the fluctuation of the energy dissipation is about 0.12. This value is very close to $\mu/3$ predicted by some early workers in turbulence.⁽⁷⁾ The μ is hypothesized to be about 0.41 by many authors.⁽¹³⁾ It was suggested⁽⁴⁻⁶⁾ that the defect for the five-thirds law should be $\mu/9$, based on the assumption of Kolmogorov’s log-normal distribution for kinetic energy dissipation in their models. The results of ref. 12 showed an increase by 0.12 in the exponent of the five-thirds law (i.e., $-5/3 + \mu/3$) for the structure functions and the spectrum

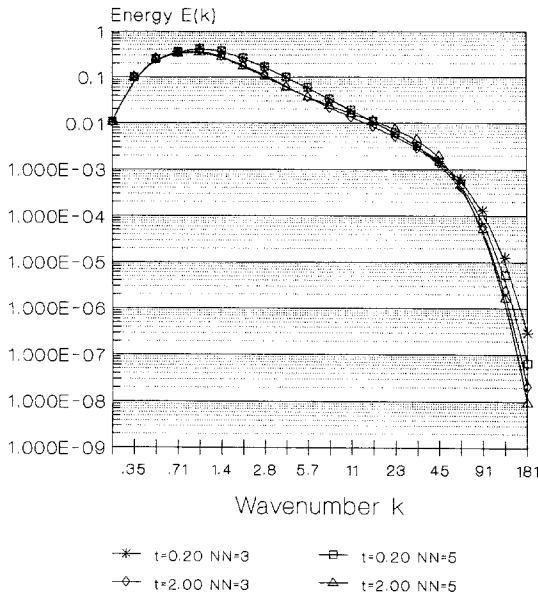


Fig. 12. Energy spectrum at (*) $t=0.20$, $NN=3$; (\square) $t=0.20$, $NN=5$; (\triangle) $t=2.00$, $NN=3$; (Δ) $t=2.00$, $NN=5$. The slope for the initial spectrum is generated by the generalized Kolmogorov spectrum formula⁽¹⁶⁾ $S(0) = -1.521$ and is taken from the inertial subrange and calculated by least-square fit from $k=2.000$ to $k=11.314$. Reynolds number $Re=1000$. NN is the parameter in the program that controls the renormalization frequency. $NN=3$ represents that renormalization occurs at every other time step; $NN=5$ represents that renormalization occurs at every four time steps.

of turbulence. However, other authors predicted that there should be a decrease in the exponent (i.e., $-5/3 - \mu/9$ or $-5/3 - \mu/3$). After comparing the above three different predictions with measured data in ref. 14, we found (as has been observed before) that one cannot tell which one of the three is best fitted by the data given the accuracy of the measurements reported.

The (very small) effect of our renormalization scheme on the final form of the energy spectrum was examined by runs with smaller Reynolds numbers and various renormalization rates. The results and discussion are included in the Appendix.

We have also developed a set of equations and program code that will calculate the fourth-order longitudinal structure function which is more sensitive to the Kolmogorov defect, $D_{LLLL}(r) = \langle [u_L(M') - u_L(M)]^4 \rangle = \langle (u' - u)^4 \rangle$, where $M' = x + r$, $M = x$, and r is the separation distance of the two points, and $u_L(M')$ and $u_L(M)$ are the components of the fluctuating velocity at the two points in the direction of the separation. We

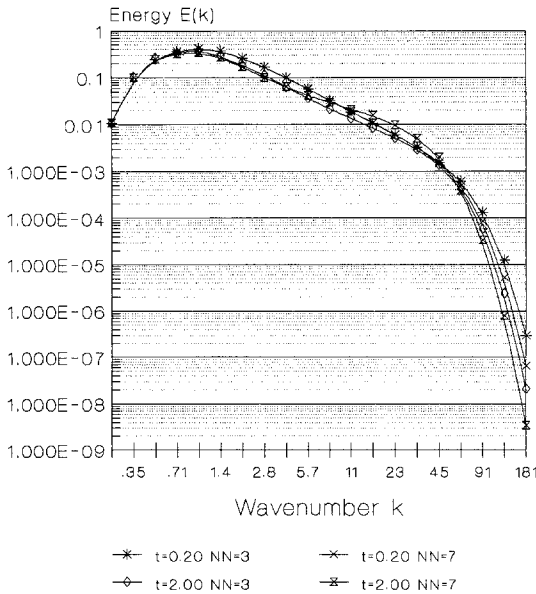


Fig. 13. Energy spectrum at (*) $t=0.20$, $NN=3$; (\times) $t=0.20$, $NN=7$; (\diamond) $t=2.00$, $NN=3$; (\times) $t=2.00$, $NN=7$. The slope for the initial spectrum is generated by the generalized Kolmogorov spectrum formula⁽¹⁶⁾ $S(0) = -1.521$ and is taken from the inertial subrange and calculated by least-square fit from $k=2.000$ to $k=11.314$. Reynolds number $Re = 1000$. NN is the parameter in the program that controls the renormalization frequency. $NN = 3$ represents that renormalization occurs at every other time step. $NN = 7$ represents that renormalization occurs at every six time steps.

have not yet obtained results for the fourth-order longitudinal structure function, which in ref. 15 is claimed necessary for obtaining a distinguishable experimental defect (from the five-thirds law).

APPENDIX. THE EFFECT OF RENORMALIZATION ON THE SLOPE OF THE ENERGY SPECTRUM IN THE INERTIAL SUBRANGE

Current results of high-Reynolds-number runs were renormalized at every second dimensionless time step. Renormalization less often than this results in a hump in the mid- to large-wavenumber range of the energy spectrum, which, because of worsening convergence, produces unreliable results. To find out the influence of our renormalization scheme on the final spectrum, we ran the program with smaller Reynolds numbers, such as 1000 and 800. Hogge⁽¹⁶⁾ obtained reasonably good results using Reynolds numbers of this order.

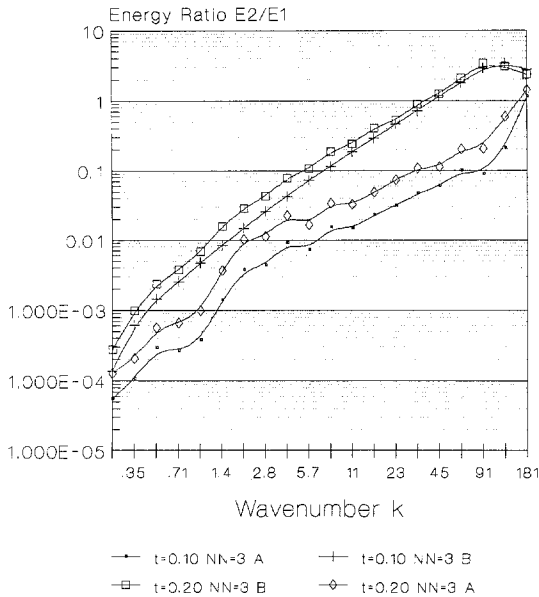


Fig. 14. Energy ratio at (·) $t=0.10$, after renormalization; (+) $t=0.10$, before renormalization; (□) $t=0.20$, before renormalization; (◇) $t=0.20$, after renormalization. The slope for the initial spectrum is generated by the generalized Kolmogorov spectrum formula⁽¹⁶⁾ $S(0) = -1.521$ and is taken from the inertial subrange and calculated by least-square fit from $k = 2.000$ to $k = 11.314$. Reynolds number $Re = 1000$. The parameter in the program that controls the renormalization frequency $NN = 3$, i.e., renormalization occurs at every other time step.

Results from runs for Reynolds number 1000 with an initial spectrum similar to Kolmogorov's generalized spectrum type⁽¹⁶⁾ show that the renormalization has little influence on the slope of the energy spectrum in the inertial subrange (see Figs. 11–13). The calculated inertial range slopes before and right after the renormalization are the same. The slopes at the corresponding time step following renormalization are different by only 0.3–0.5% between runs with or without renormalization, among the bulk of our results. Figures 11–13 show a series of spectra with different renormalization rates. The slope for the initial spectrum was generated by the generalized Kolmogorov spectrum formula, $S(0) = -1.521$. The slope is taken from the inertial subrange and calculated by least-square fit. The Reynolds number is 1000. NN – 1 in these figures stands for the rate of renormalization. NN = 3 means that renormalization occurs at every second dimensionless time step, NN = 5 means that renormalization occurs at every fourth dimensionless time step, and NN = 7 means we renormalize the run every six dimensionless time steps.

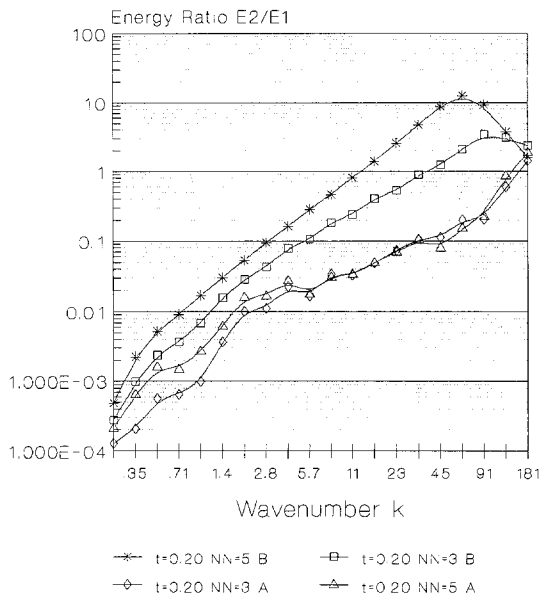


Fig. 15. Energy ratio at $t = 0.20$. The slope for the initial spectrum is generated by the generalized Kolmogorov spectrum formula⁽¹⁶⁾ $S(0) = -1.521$ and is taken from the inertial subrange and calculated by least-square fit from $k = 2.000$ to $k = 11.314$. Reynolds number $Re = 1000$. (*) NN = 5, before renormalization, (□) NN = 3, before renormalization, (◇) NN = 3, after renormalization, (△) NN = 5, after renormalization. NN is the parameter in the program that controls the renormalization frequency. NN = 5 represents that renormalization occurs at every four time steps. NN = 3 represents that renormalization occurs at every other time step.

However, the ratio between the second term of the energy spectrum $E_2(k)$ and the so-called Gaussian part of the energy spectrum $E_1(k)$ is drastically changed (see Figs. 14 and 15). This is because we redistribute the energy in such a way that most of the energy would be concentrated in the Gaussian part while retaining the spectrum itself: the measure-preserving transformation. Figures 14 and 15 show the ratio between the energy correction term E_2 and the energy Gaussian term E_1 . In these figures results are given for both before renormalization and after renormalization for the same time step. From these ratios we see that energy transfer from the Gaussian term to the correction term is so fast that at a fourth dimensionless time step before renormalization, with $NN = 5$, we will have eight k -value terms such that $E_2(k) \geq E_1(k)$. Such is not the case for $NN = 3$ runs, which renormalize every two dimensionless time steps, and have only four to five k -value terms that show $E_2(k) \geq E_1(k)$.

Comparison between runs with different renormalization rates shows that the less often we renormalize the run, the less reliable are the results we get, due to the fact that at the large-wavenumber end, more and more terms of $E_2(k)$ exceed the corresponding terms in $E_1(k)$ because of poor convergence. We must stop the procedure at a certain time step and redistribute the energy. At a sixth dimensionless time step without renormalization we would have 10 k -value terms in the spectrum such that $E_2(k) \geq E_1(k)$, making the inertial subrange results unreliable.

REFERENCES

1. G. K. Batchelor, *Theory of Homogeneous Turbulence* (Cambridge University Press, New York, 1963).
2. L. D. Landau and E. M. Lifshitz, *Fluid Mechanics* (Pergamon Press, London, 1963).
3. A. N. Kolmogorov, *J. Fluid Mech.* **13**:82 (1962).
4. A. M. Yaglom, *Dokl. Akad. Nauk SSSR, Fiz. Atmos. Okeana* **3**:26 (1966).
5. E. A. Novikov, *Prikl. Mat. Mekh.* **35**:266 (1970).
6. B. Mandelbrot, Turbulence and Navier-Stokes equations, *Lecture Notes Math.* **565**:121 (1976).
7. U. Frisch, P. L. Sulem, and M. Nelkin, *J. Fluid Mech.* **87**:7 (1978).
8. H. D. Hogge and W. C. Meecham, *J. Fluid Mech.* **85**:325 (1978).
9. W. C. Meecham and D. T. Jeng, *J. Fluid Mech.* **32**:225 (1968).
10. M. Doi and T. Imamura, *Prog. Theor. Phys.* **41**:358 (1969).
11. S. E. Bodner, *Phys. Fluids* **12**:33 (1969).
12. T. C. Chung and W. C. Meecham, APS 37th Meeting of Division of Fluid Dynamics, Rhode Island, November 18–20, 1984, *Phys. Rev.*
13. A. S. Gurvich and S. L. Zubkovskii, *Izv. Akad. Nauk SSSR, Ser. Geofiz.* **12**:1856 (1963).
14. H. L. Grant, R. W. Stewart, and A. Moilliet, *J. Fluid Mech.* **12**:241 (1961).
15. C. W. Van Atta and W. Y. Chen, *J. Fluid Mech.* **44**:145 (1970).
16. H. D. Hogge, "The Wiener-Hermite Expansion Applied to Decaying Turbulence Using a Renormalized Time-Dependent Base," Ph.D. thesis, University of California at Los Angeles, Los Angeles, California (1977).